RSC Advances

PAPER

View Article Online
View Journal | View Issue

A nano-sized solid acid synthesized from rice hull ash for biodiesel production

Cite this: *RSC Adv.*, 2014, **4**, 20535

Danlin Zeng,* Shenglan Liu, Wanjun Gong, Hongxiang Chen and Guanghui Wang

Received 10th January 2014
Accepted 9th April 2014

DOI: 10.1039/c4ra00266k

www.rsc.org/advances

A nano-sized solid acid was synthesized from rice hull ash by acid activation. The solid acid was characterized by XRD, FT-IR, TEM and solid-state NMR spectroscopy. The characterization results show that the solid acid is amorphous silica with –OH and $-SO_3H$ functional acid groups. The TEM images show that the particle size range of the solid acid catalyst is 50–100 nm. In addition, the catalytic results indicate that the solid acid exhibits excellent activity and recyclability for the transesterification reaction of soybean oil with methanol, suggesting promising industrial applications in biodiesel production.

1. Introduction

Liquid acids (H_2SO_4, HF or H_3PO_4) generate serious problems such as dangerous transportation, difficult separation, waste acid pollution and strong corrosivity in industrial application.[1–4] Though the base-catalyzed transesterification is relatively faster than the acid-catalyzed transesterification, the base catalyst is sensitive to the oils with high free fatty acid (FFA) content, which greatly limits the raw materials of biodiesel.[5] Consequently, the research on solid acid catalysts has been paid considerable attention in acid catalysis because of their environmental, economical and operational advantages.[6] In the past decades, several solid acids have been synthesized and used in acid catalysis reactions. Inorganic-oxide solids such as zeolites,[7] niobic acid,[8,9] strong acidic ion exchange resins,[10,11] sulfonated zirconia and carbon-based materials are the typical solid acids that have been extensively investigated.[12–15] These solid acids have attracted a great deal of attention due to their easy operation, good catalytic efficiency and high selectivity in the catalysis reaction. One useful example of a reusable heterogeneous solid acid is silica sulfuric acid, which exhibits excellent efficiency in lots of acid catalysis reactions.[16,17] This solid acid can be easily synthesized from the treatment of silica gel at moderate temperature.[18]

Rice hull, an agro-based waste, is normally disposed of by burning in the field, which results in environmental pollution in China. Rice hull ash (RHA) prepared by calcination of rice hull under air was been found to be an economically viable raw material for the production of silicates and silica.[19–22] It is necessary to explore the possibility of using this low cost silica to prepare solid acid for heterogeneous catalysis.

In this work, rice hull ash was used as the starting material to prepare silica-based solid acid catalyst for biodiesel production from soybean oil and methanol. A nano-sized solid acid was synthesized from rice hull ash by NaOH leaching and concentrated H_2SO_4 activation. The solid acid catalyst was also characterized by X-ray diffraction (XRD), Fourier-transform infrared spectroscopy (FT-IR), transmission electron microscopy (TEM) and solid state nuclear magnetic resonance (NMR) spectroscopy. The characterization results will be helpful for obtaining fundamental information of the roles of surface functional groups in the solid acid, which is crucial in the design of a novel silica-based solid acid for industrial application.

2. Experimental

2.1. Catalyst preparation

2.1.1 Solid acid from rice hull ash. Rice hull was obtained from a grain depot in Wuhan, China. Rice hull was heated at 10 °C min^{-1} in three-stages, first to 150 °C and held for 1 h, then to 325 °C and held for another 1 h, and finally to 575 °C and held for 10 h in air to remove the organics and resultant carbon. The product, in the form of white ash, was collected, sealed in a plastic bottle and stored at room temperature for the following experiment and analysis. Table 1 lists the chemical composition of the rice hull ash, which was determined by atomic emission measurements using inductively coupled plasma (ICP) emission spectroscopy (Spectro Analytical Instruments).

NaOH solution (1 M) was added to the rice hull ash samples with a solid to liquid ratio of 1 : 5 and boiled for 1 h with constant stirring to dissolve the silica and produce a sodium

Table 1 Chemical composition of rice hull ash (wt%)

Sample	SiO_2	CaO	Na_2O	Al_2O_3	MgO
Rice hull ash	90.15	0.84	0.70	0.26	0.05

College of Chemical Engineering and Technology, Hubei Key Laboratory of Coal Conversion and New Carbon Material, Wuhan University of Science and Technology, Wuhan 430081, China. E-mail: zdanly@163.com; Fax: +86 27 6886 2181; Tel: +86 27 6886 2181

silicate solution. The solutions were filtered and then washed with 100 mL of boiling water. The filtrates and washings were allowed to cool to room temperature and were titrated with 0.1 M HNO_3 with constant stirring to pH 7. Silica gels started to precipitate slowly when the pH was decreased. The produced silica gels were aged for 12 h, centrifuged, and then transferred into a beaker and dried at 150 °C for 12 h to produce silica. A silica sample calcined at 1000 °C for 12 h was also prepared to characterize its phase transformation.

To prepare the solid acid, the silica gels (SiO_2, 99.6 wt%; calcined at 150 °C) were activated with concentrated H_2SO_4 (98 wt%) at 200 °C under a N_2 flow (10 mL min^{-1}) for 10 h at a ratio of solid to liquid of 1 g : 100 mL. At last, the mixture was diluted with deionized water, filtered, washed thoroughly, and dried at 150 °C for 12 h to obtain the solid acid catalyst (SiO_2, 99.0 wt%). All the samples were stored in airtight plastic bottles.

2.1.2 SO_4^{2-}/ZrO_2 catalyst. As a typical solid acid, SO_4^{2-}/ZrO_2 catalyst was used to perform a comparative study. The SO_4^{2-}/ZrO_2 catalyst in this work was prepared using the classic two-step method.[23] Zirconium hydroxide was prepared by hydrolysis of zirconyl chloride ($ZrOCl_2 \cdot H_2O$, 99%, Merk) with aqueous ammonia, and then the SO_4^{2-}/ZrO_2 catalyst was prepared by an impregnation method. Zirconium hydroxide fractions were soaked in 1 M sulfuric acid solution with stirring for 1 h at room temperature. The H_2SO_4-impregnated zirconium hydroxide sample was dried at 400 °C in air for 24 h to obtain the SO_4^{2-}/ZrO_2 catalyst.

2.2. Sample characterization

The concentration of acid sites on the catalysts was determined by a titration method in aqueous solution. One gram of the sample was placed in 50 mL of 0.05 M NaOH solution. The vials were sealed and shaken for 24 h. Then 5 mL of the filtrate was pipetted, and the excess base was titrated with HCl. The numbers of acidic sites were calculated from the amount of NaOH that reacted with the catalyst.

The surface area and porosity properties of samples were evaluated by N_2 adsorption–desorption isotherms carried out at 77 K on a Micromeritics ASAP 2020 sorption analyzer. Prior to the adsorption–desorption measurements, all the samples were degassed at 150 °C in N_2 flow (50 mL min^{-1}) for 12 h.

The FT-IR spectra were recorded on an Impact 410 Nicoletspectrometer with a resolution of 2 cm^{-1}. Twelve milligrams of each sample was pressed into a self-supported 16 mm diameter wafer. The wafers were heated at 200 °C in an IR cell under vacuum (<10^{-3} Pa) for 4 h before the IR spectra of the samples were measured.

X-ray diffraction (XRD) was performed with a Philips X'PERT-Pro-MPD diffractometer, operating with Cu Kα radiation (40 kV, 30 mA) and Ni filter.

The TEM (transmission electron microscopy) images were taken with a JEOL JEM-2000EX instrument operated at 80 kV.

All the NMR experiments were carried out at 9.4 T on a Varian Infinityplus-400 spectrometer with resonance frequencies of 400.12, 100.4, and 161.9 MHz for ^1H, ^{13}C, and ^{31}P, respectively. The 90° pulse widths for ^1H, ^{13}C, and ^{31}P were measured to be 3.7, 4.4, and 3.6 μs, respectively. The chemical shifts were referenced to tetramethylsilane (TMS) for ^1H, to hexamethylbenzene (HMB) for ^{13}C, and to 85% H_3PO_4 solution for ^{31}P. Repetition times of 6 s for ^1H and 60 s for ^{31}P single-pulse experiments were used. The magic angle spinning rate was 5 kHz.

For the adsorption of probe molecules of trimethylphosphine (TMP), samples were kept at 673 K under the vacuum less than 1×10^{-3} Pa for at least 8 h. The adsorption of TMP was performed at room temperature with a loading of about 0.1 mmol per gram catalyst. The adsorption procedure of trimethylphosphine oxide (TMPO) was different from that of TMP. About 0.5 g of dehydrated sample was mixed with 3 mL CH_2Cl_2 solution containing 0.1 M TMPO in a glove box before the mixture was stirred for 3 h by an ultrasonic shaker, equilibrated for 5 h, and then evacuated under vacuum to remove CH_2Cl_2 and excess TMPO before NMR measurements.

2.3. Procedure for biodiesel synthesis

2.3.1 Soybean oil. Food-grade soybean oil supplied by a commercial supermarket was used to carry out the transesterification reaction. According to GC (HP6890) analysis, the fatty acid compositions of the used soybean oil were as follows: palmitic acid, 12.5 wt%; stearic acid, 5.9 wt%; oleic acid, 26.6 wt %; linoleic acid, 49.9 wt%; and linolenic acid, 5.4 wt%. The water content of the oil was reduced to lower than 10 ppm. The average molecular weight of the oil is 850.

2.3.2 Transesterification. The transesterification of soybean oil with methanol was carried out by using the solid acid catalyst prepared from rice hull ash. A 250 mL glass flask with a water-cooled condenser was charged with 8.74 g (10.0 mmol, calculated from the average molecular weight of soybean oil) of soybean oil, 3.84 g of anhydrous methanol (120 mmol) and 0.015 g of the catalyst. The mixture was vigorously stirred with a magnetic stirrer. All of the transesterification reactions were performed under reflux, with vapor from the reaction mixture being condensed by cold water (about 10 °C). After the transesterification reaction finished, the mixture was filtered and the residual methanol was separated from the liquid phase *via* rotary evaporation.

2.3.3 Analysis. Analysis of the reaction mixtures was carried out in a HP 6890 series gas chromatograph equipped with a flame ionization detector (FID). The solgel premium capillary column (30 m × 0.25 mm × 0.25 μm) was used in the analysis. At first, the oven was kept at 180 °C for 5 min and then the temperature was increased to 210 °C at a rate of 3 °C min^{-1}. The injection volume of all the samples was 0.2 μL. The inlet temperature was 250 °C, and the detector temperature was 270 °C. TOF (turn over frequency) was calculated based on the data of the moles of converted reactant, the moles of acid sites and the reaction equilibrium time.

2.3.4 Recycling. Recycling experiments were performed to determine the catalytic stability of the solid acid catalysts. The same catalyst was used in a number of cycles without any treatment between the cycles. The spent solid acid was obtained after 10 recycle times. Then the spent solid acid was washed

Table 2 Pore structure and total acid density of rice hull ash and solid acid obtained from rice hull ash (fresh, spent and regenerated)[a]

Sample	S_{BET} ($m^2\ g^{-1}$)	V_{tot} ($cm^3\ g^{-1}$)	D (nm)	Total acid density (mmol g^{-1})
Rice hull ash	49	0.023	0.58	0.01
Solid acid (fresh)	203	0.756	2.16	4.05
Solid acid (spent)	143	0.549	2.01	2.32
Solid acid (regenerated)	199	0.735	2.11	3.96

[a] S_{BET}, specific surface area from BET method; V_{tot}, total pore volume; D, average pore diameter.

with acetone and dried at 120 °C under vacuum for 5 h to obtain the regenerated solid acid. The pore structures and total acid densities of rice hull ash and solid acid from rice hull ash (fresh, spent and regenerated) are listed in Table 2.

3. Results and discussion

3.1. Catalyst characterization

3.1.1 XRD analysis. Fig. 1 illustrates the XRD patterns of the rice hull ash, silica from rice hull ash and the solid acid. The broad diffraction peaks arising at around $2\theta = 22.5$ for rice hull ash, silica (calcined at 150 °C) and solid acid corresponded to the diffraction of amorphous silica.[24] The sharp smaller peaks observed for the rice hull ash were due to the presence of impurities in the sample.[25] The peaks ($2\theta = 26.72$, 32.50, 39.29 and 46.50, due to crystalline silica) in the XRD pattern of silica from the rice hull ash (Fig. 1c) indicate that crystalline silica can be produced from the rice hull ash by calcination at a relatively higher temperature.[26] Other reports have confirmed that phase transformation occurs at higher calcination temperatures, which is consistent with the present case.[27,28] Due to its high surface area, the amorphous silica (calcined at 150 °C) was chosen as the raw material for the solid acid. As can be seen in the XRD characterization (Fig. 1d), the solid acid catalyst here is clearly in the form of amorphous silica.

3.1.2 FT-IR analysis. The major chemical groups present in silica are identified by the FTIR spectra shown in Fig. 2. The band at 465 cm^{-1} is attributed to the bending vibrations of Si–O–Si. The bands at 831 and 1098 cm^{-1} are ascribed to the Si–O– symmetric and asymmetric stretching modes, respectively,[29]

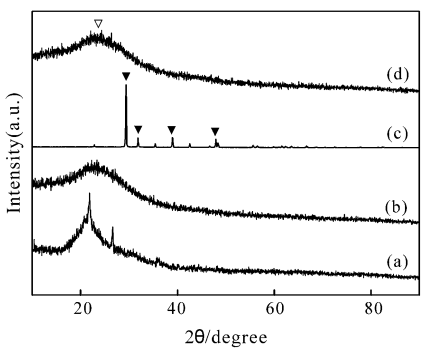

Fig. 1 XRD patterns of (a) rice hull ash, (b) silica (calcined at 150 °C), (c) silica (calcined at 1000 °C) and (d) the solid acid. ▼ denotes peaks of crystalline silica, ▽ denotes peak of amorphous silica.

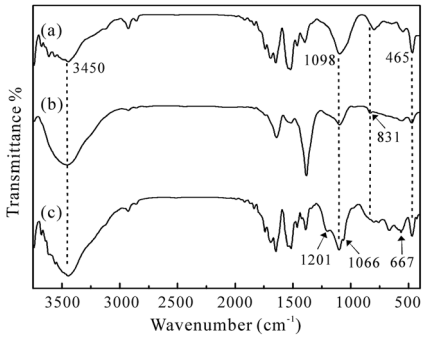

Fig. 2 FT-IR spectra of (a) rice hull ash, (b) silica (calcined at 150 °C) and (c) the solid acid.

while the bands at 1066 and 1201 cm^{-1} in the spectra of the solid acid can be assigned to the SO_2 asymmetric and symmetric stretching modes, respectively.[30] The band at 667 cm^{-1} can be attributed to the chelating structure of SO_4^{2-} groups.[18] This indicates that SO_4^{2-} groups are not in the free sulfuric acid state but linked on the surface of the activated solid acid. The broad band centered at 3450 cm^{-1} was assigned to the –OH stretching mode.[31] Therefore, the FT-IR results confirm that all the three samples consist of the silica particles. In addition, the $-SO_3H$ groups were formed as the functional groups in the solid acid after sulfuric acid activation.

3.1.3 Solid state NMR analysis. The type and strength of acid sites are the fundamental properties of the solid acid. Trimethylphosphine (TMP) is a very useful probe molecule in authenticating the acid types such as Lewis or Brønsted acid sites in the solid acid surface.[23] Fig. 3a illustrates the ^{31}P single pulse spectrum obtained after adsorbing TMP onto the surface of solid acid. Two peaks at −2 and −60 ppm are observed in the spectrum. The former can be unambiguously assigned to TMP adsorbed on the Brønsted acid sites, and the latter generally originates from physisorbed TMP. It is obvious that a negligible amount of Lewis sites exists in the solid acid since no signal appears between −32 and −58 ppm.[32] Since no Lewis acid sites were detected by the TMP probe molecule and the resonance at 45 ppm is ascribed to the physisorbed trimethylphosphine oxide (TMPO),[33] the other two resonances at 55 and 72 ppm in the ^{31}P NMR spectrum of TMPO adsorbed on the solid acid can be both attributed to the Brønsted sites (Fig. 3b): the weakly acidic OH groups and the relatively strong acid site $-SO_3H$ groups, respectively.[34] The large chemical shift of 72 ppm indicates that the acid strength of the solid acid is higher than

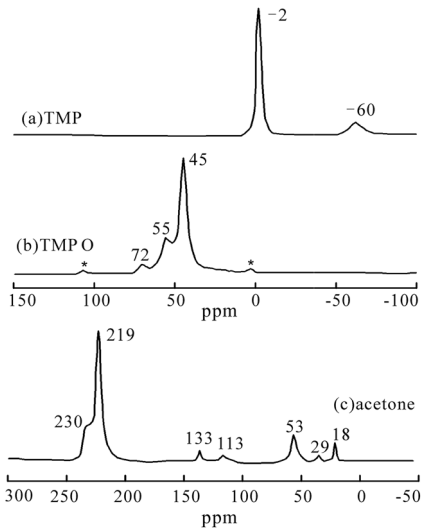

Fig. 3 ^{31}P single pulse with ^{1}H decoupling MAS spectra of (a) TMP and (b) TMPO adsorbed on the solid acid; (c) ^{13}C CP/MAS NMR spectra of 2-^{13}C-acetone (0.2 mmol g^{-1}) adsorbed on the solid acid. The asterisk denotes spinning sidebands.

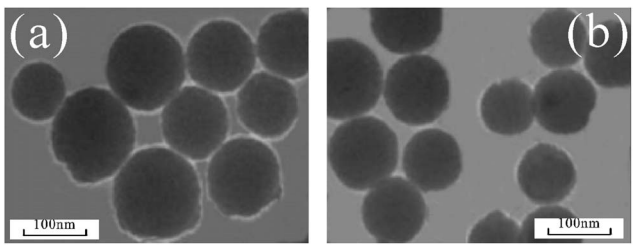

Fig. 4 TEM of (a) silica (calcined at 150 °C) and (b) the solid acid.

that of HY with the Si/Al ratio of 3 (shown ^{31}P chemical shifts of 65 ppm).[35] As a reliable NMR probe molecule, 2-^{13}C-acetone can be used in conjunction with the ^{13}C MAS NMR chemical shift as a measure of the relative acid strength of various solid acids.[35] The formation of a hydrogen bond between the acidic proton and the carbonyl oxygen of adsorbed acetone will cause a downfield shift of the carbonyl carbon. Besides the peaks associated with mesityl oxide (133, 53, 29 and 18 ppm),[36] two peaks at 219 and 230 ppm are observed in the ^{13}C CP/MAS spectrum of acetone-2-^{13}C adsorbed on the solid acid (Fig. 3c). The resonance at 113 ppm is due to the background of the probe. Similarly, the signal at 219 ppm is ascribed to acetone-2-^{13}C adsorbed on the relatively weak acidic –OH groups, and the resonance at 230 ppm is due to acetone-2-^{13}C adsorbed on the strong Brønsted acid sites (–SO_3H groups). The signal of 230 ppm indicates that the acid strength of the solid acid is weaker than that of 100% H_2SO_4 (a ^{31}C chemical shift of 245 ppm).[37]

3.1.4 TEM. The nano-size and spherical structure of silica from the rice hull ash and the solid acid were confirmed by transmission electron microscopy (TEM) images (Fig. 4). As Fig. 4 shows, particles of the two samples were spherical with a diameter of about 50–100 nm, which indicates that the solid acid is a nano-sized catalyst.

3.2. Catalytic reaction

In order to evaluate the activity of the solid acid in the reaction, a comparative study was carried out between the solid acid prepared from rice hull ash, concentrated H_2SO_4 and the typical solid acid SO_4^{2-}/ZrO_2 catalyst (Table 3). The reaction used was the transesterification of soybean oil (10 mmol) with methanol (120 mmol) under reflux. The same amount (0.015 g) of all the catalysts was used in the reactions. As can be seen in Table 3, the solid acid from rice hull ash shows lower activity than that of concentrated H_2SO_4, but still higher than that of the SO_4^{2-}/ZrO_2 catalyst. It clearly suggests that the solid acid should be considered as one of the best choices for an economically convenient, user-friendly catalyst for acid catalysis reaction.

The catalytic reusability of the solid acid from rice hull ash was evaluated by running the transesterification reaction 10 times. The same catalyst was directly used each time without any pretreatment. As shown in Fig. 5, the yield of biodiesel gradually decreased from 92% to 51% in the 10 cycles. From

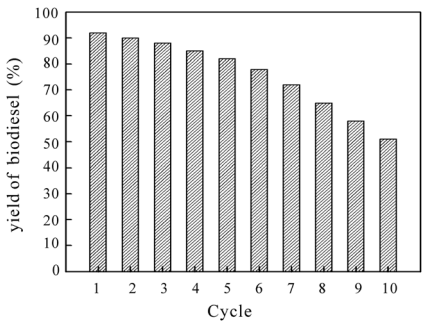

Fig. 5 The recycling of the solid acid from rice hull ash for the transesterification reaction. Reaction conditions: 10 mmol soybean oil; 120 mmol methanol; 0.015 g catalyst; 80 °C.

Table 3 Textural properties and catalytic performance of the various catalysts[a,b,c]

Catalysts	S_{BET} (m^2 g^{-1})	V_{tot} (cm^3 g^{-1})	D (nm)	Total acid density (mmol g^{-1})	Yield (%)	TOF (h^{-1})
Solid acid	203	0.246	1.16	4.05	92	75.7
SO_4^{2-}/ZrO_2	155	0.224	4.88	4.42	87	65.6
H_2SO_4 (98%)	—	—	—	20.40	96	125.5

[a] S_{BET}, specific surface area from BET method; V_{tot}, total pore volume; D, average pore diameter. [b] TOF (turn over frequency) was calculated based on the data of the moles of converted reactant, the moles of acid sites and reaction equilibrium time. [c] Reaction conditions: 10 mmol soybean oil; 120 mmol methanol; 0.015 g catalyst; 80 °C.

Table 2 we can see that the loss in surface area, pore volume and acid sites of the spent catalyst suggests that deactivation arises as a result of pore blocking by some reaction intermediate or product species. When the 10 cycles were over, the spent catalyst was obtained, and then the regeneration process was performed to reactivate the spent catalyst. After washing with acetone and then drying at 120 °C under vacuum for 5 h, the total acid density increased from 2.32 to 3.96 mmol g^{-1}. It mostly recovered its original activity (4.05 mmol g^{-1} of fresh catalyst), which confirms its reusability as a catalyst for biodiesel production (Table 2).[38] Therefore, the simple regeneration method is helpful for the catalyst's application in a fixed bed of a continuous product system.

4. Conclusions

In summary, a nano-sized solid acid was synthesized from rice hull ash by acid activation. Our characterization results show that the solid acid is amorphous silica with –OH and $–SO_3H$ functional acid groups. The TEM images show that the particle size range of the solid acid catalyst is 50–100 nm. The catalytic results indicate that the solid acid catalyst is very active at suitable conditions for the transesterification of soybean oil with methanol. The reusability of the solid acid was also confirmed in the transesterification reaction. It is possible that this promising solid acid can be widely used in the acid catalysis reaction.

Acknowledgements

We acknowledge financial support from the Science and Technology Plan of Wuhan (201060723317), the Open Research Fund of Hubei Key Laboratory for Efficient Utilization and Agglomeration of Metallurgic Mineral Resources and the Open Research Fund of Key Laboratory for Ferrous Metallurgy and Resources Utilization of Ministry of Education (FMRU201209).

References

1 P. T. Anastas and M. M. Kirchhhoff, *Acc. Chem. Res.*, 2002, **35**, 686–694.
2 J. M. Desimone, *Science*, 2002, **297**, 799–803.
3 P. T. Anastas and J. B. Zimmermann, *Environ. Sci. Technol.*, 2003, **37**, 94–101.
4 E. Lotero, Y. Liu, D. E. Lopez, A. Suwannakaran, D. A. Bruce and J. G. Goodwin, *Ind. Eng. Chem. Res.*, 2005, **44**, 5353–5363.
5 A. P. S. Chouhan and A. K. Sarma, *Renewable Sustainable Energy Rev.*, 2011, **15**, 4378–4399.
6 A. Corma and H. Garcia, *Catal. Today*, 1997, **38**, 257–308.
7 T. Okuhara, *Chem. Rev.*, 2002, **102**, 3641–3666.
8 J. A. Melero, J. Iglesias and G. Morales, *Green Chem.*, 2009, **11**, 1285–1308.
9 A. Corma and A. Martinez, *Adv. Mater.*, 1995, **7**, 137–144.
10 M. A. Harmer and Q. Sun, *Appl. Catal., A*, 2001, **221**, 45–62.
11 M. A. Harmer, Q. Sun, A. J. Vega, W. E. Farneth, A. Heidekum and W. F. Hoelderich, *Green Chem.*, 2000, **2**, 7–14.
12 A. A. Kiss, A. C. Dimian and G. Rothenberg, *Adv. Synth. Catal.*, 2006, **348**, 75–81.
13 V. L. Budarin, J. H. Clark, R. Luque and D. J. Macquarrie, *Chem. Commun.*, 2007, 634–636.
14 S. Suganuma, K. Nakajima, M. Kitano, D. Yamaguchi, H. Kato, S. Hayashi and M. Hara, *J. Am. Chem. Soc.*, 2008, **130**, 12787–12793.
15 D. Zeng, S. Liu, W. Gong, G. Wang, J. Qiu and Y. Tian, *Catal. Commun.*, 2013, **40**, 5–8.
16 J. M. Riego, Z. Sedin, J. M. Zaldlvar, N. C. Marzianot and C. Tortatot, *Tetrahedron Lett.*, 1996, **37**, 513–516.
17 S.-N. Masoud and J. Jaber, *Comb. Chem. High Throughput Screening*, 2012, **15**, 705–712.
18 H. R. Shaterian, M. Ghashang and M. Feyzi, *Appl. Catal., A*, 2008, **345**, 128–133.
19 S. R. Kamath and A. Proctor, *Cereal Chem.*, 1998, **75**, 484–487.
20 V. P. Della, I. Kühn and D. Hotza, *Mater. Lett.*, 2002, **57**, 818–821.
21 T. Witoon, M. Chareonpanich and J. Limtrakul, *Mater. Lett.*, 2008, **62**, 1476–1479.
22 S. Huang, S. Jing, J. F. Wang, Z. W. Wang and Y. Jin, *Powder Technol.*, 2001, **117**, 232–238.
23 J. F. Haw, J. H. Zhang, K. Shimizu, T. N. Venkatraman, D. Luigi, W. Song, D. H. Barich and J. B. Nicholas, *J. Am. Chem. Soc.*, 2000, **122**, 12561–12570.
24 X. Ma, B. Zhou, W. Gao, Y. Qu, L. Wang, Z. Wang and Y. Zhu, *Powder Technol.*, 2012, **217**, 497–501.
25 U. Kalapathy, A. Proctor and J. Shultz, *Bioresour. Technol.*, 2002, **85**, 285–289.
26 M. Kima, S. H. Yoon, E. Choic and B. Gil, *LWT–Food Sci. Technol.*, 2008, **41**, 701–706.
27 M. Sarangi, P. Nayak and T. N. Tiwari, *Composites, Part B*, 2011, **42**, 1994–1998.
28 H. Hamdan, M. N. M. Muhid, S. Endud, E. Listiorini and Z. Ramli, *J. Non-Cryst. Solids*, 1997, **211**, 126–131.
29 V. S. Braga, J. A. Dias, S. C. L. Dias and J. L. Macedo, *Chem. Mater.*, 2005, **17**, 690–695.
30 W. Zhao, B. Yang, C. Yi, Z. Lei and J. Xu, *Ind. Eng. Chem. Res.*, 2010, **49**, 12399–12404.
31 W. P. Rothwell, W. Shen and J. H. Lunsford, *J. Am. Chem. Soc.*, 1984, **106**, 2452–2453.
32 J. H. Lunsford, W. P. Rothwell and W. Shen, *J. Am. Chem. Soc.*, 1985, **107**, 1540–1547.
33 E. F. Rackiewicz, A. W. Peters, R. F. Wormsbecher, K. J. Sutovich and K. T. Mueller, *J. Phys. Chem. B*, 1998, **102**, 2890–2896.
34 Q. Zhao, W. H. Chen, S. J. Huang, Y. C. Wu, H. K. Lee and S. B. Liu, *J. Phys. Chem. B*, 2002, **106**, 4462–4469.
35 J. F. Haw, J. B. Nicholas, T. Xu, L. W. Beck and D. B. Ferguson, *Acc. Chem. Res.*, 1996, **29**, 259–267.
36 T. Xu, E. J. Munson and J. F. Haw, *J. Am. Chem. Soc.*, 1994, **116**, 1962–1972.
37 A. I. Biaglow, R. J. Gorte and D. White, *J. Catal.*, 1994, **150**, 221–224.
38 B. A. D. Neto, M. B. Alves, A. A. M. Lapis, F. M. Nachtigall, M. N. Eberlin, J. Dupont and P. A. Z. Suarez, *J. Catal.*, 2007, **249**, 154–161.